

Rosuvastatin protects against endothelial cell apoptosis *in vitro* and alleviates atherosclerosis in ApoE^{-/-} mice by suppressing endoplasmic reticulum stress

JIANAN GENG¹, HUALI XU¹, WENWEN FU¹, XIAOFENG YU¹, GUOLIANG XU²,
HONGYAN CAO², GUANGZHU LIN² and DAYUN SUI¹

¹Department of Pharmacology, School of Pharmaceutical Sciences, Jilin University, Changchun, Jilin 130021;

²Department of Cardiovascular Medicine, the Eastern Division of First Hospital, Jilin University, Changchun, Jilin 130031, P.R. China

Received November 11, 2019; Accepted April 1, 2020

DOI: 10.3892/etm.2020.8733

Abstract. The development of abnormal lipid-induced atherosclerosis is initiated with endothelial cell apoptosis. Vascular endothelial cells possess highly developed endoplasmic reticulum (ER), which is involved in lipid metabolism, indicating that ER stress may contribute chiefly to the induction of endothelial cell apoptosis. Based on its ability to reduce cholesterol levels, rosuvastatin may play an endothelial and vascular protective role by regulating ER stress. In the present study, the involvement of the inhibition of the ER stress-induced endothelial injury was investigated in combination with the lipid lowering effects of rosuvastatin. This compound can be used to inhibit cholesterol synthesis in atherosclerosis. Rosuvastatin decreased the apoptotic rates of human umbilical vascular endothelial cells (HUVECs) that had been stimulated with ox-low density lipoprotein (LDL) *in vitro* and repressed the mRNA levels of *CHOP*, *sXBP1* and *caspase-12*, and decreased caspase-12 activity, as well as the content of glucose-regulated protein 78 (GRP78), phosphorylated (p)-protein kinase RNA-like ER kinase (PERK), p-inositol-requiring protein 1 α (IRE1 α) and p-eIF2 α proteins. In addition, ApoE^{-/-} mice were fed with atherogenic chow for 8 weeks for atherosclerosis induction and rosuvastatin was provided by intragastric administration for an additional 4 weeks. Subsequently, the atherosclerotic plaque formation

in the aorta was evaluated by Oil Red O and hematoxylin and eosin staining, and the serum LDL, high-density lipoprotein, total cholesterol (TC) and triacylglycerol (TG) levels were measured. In addition, the induction of apoptosis of endothelial cells and the expression levels of GRP78, p-PERK, p-IRE1 α and p-eIF2 α were assessed in the aorta. Rosuvastatin repressed atherosclerotic plaque formation and endothelial apoptosis in the aorta and decreased LDL and TG levels in the serum, as determined by *in vivo* results. Furthermore, it down-regulated the expression levels of protein chaperone GRP78, p-PERK, p-IRE1 α and p-eIF2 α in the aortic intima. The data indicated that rosuvastatin could protect HUVECs from ER stress-induced apoptosis triggered by oxidized LDL. It could also inhibit atherosclerosis formation in ApoE^{-/-} mice aorta by regulating the PERK/eIF2 α /C/EBP α -homologous protein and IRE1 α /sXBP1 signaling pathways. Taken collectively, the present study demonstrated the preventive and therapeutic effects of rosuvastatin in protecting from the development of endothelial cell dysfunction diseases.

Introduction

Atherosclerosis is the main cause of the development of multiple diseases, such as stroke, myocardial infarction and peripheral arterial disease (1). The dysregulation of lipid metabolism, notably the generation of oxidized (ox) low-density lipoprotein (LDL), is an important trigger for the development of atherosclerosis, causing vascular endothelial dysfunction and induction of apoptosis (2). The vascular endothelium acts as a key barrier of the vessel wall, resisting adhesion and migration of inflammatory cells, which can promote the formation of the atherogenic plaque (3). Plaque rupture leads to the development of atherosclerotic-associated complications, which are accompanied by high mortality (4). Therefore, the inhibition of endothelial cell apoptosis is important to protect from infiltration of inflammatory cells and from atherogenic plaque formation.

The endoplasmic reticulum (ER) is a key organelle and is responsible for multiple lipid metabolism, whereas ER dysfunction is considered a risk factor for chronic metabolic

Correspondence to: Professor Dayun Sui, Department of Pharmacology, School of Pharmaceutical Sciences, Jilin University, 1266 Fujin Road, Changchun, Jilin 130021, P.R. China
E-mail: suidayun@hotmail.com

Dr Guangzhu Lin, Department of Cardiovascular Medicine, the Eastern Division of First Hospital, Jilin University, 3302 Jilin Road, Changchun, Jilin 130031, P.R. China
E-mail: lingz6403@163.com

Key words: atherosclerosis, endoplasmic reticulum stress, endothelial cell apoptosis, rosuvastatin

diseases, including obesity, diabetes and insulin resistance (3). Vascular endothelial cells exhibit a high number of highly developed ER organelles, which determine their sensitivity to ER dysfunction induced by dyslipidemia and to the induction of endothelial cell apoptosis (5). ER stress is used to correct misfolded or unfolded proteins accumulating in ER, whereas it is also produced if unfolded proteins are continuously overloaded. Under these conditions, the balance and function of ER cannot be re-established, resulting in a vicious cycle that damages cells and leads to the induction of apoptosis and cytotoxicity (6). Therefore, the inhibition of ER stress induction may be one of the potential ways to protect blood vessels and inhibit atherosclerosis formation under conditions of abnormal lipoprotein metabolism.

The ER stress sensors primarily include the protein kinase RNA-like ER kinase (PERK) and the inositol-requiring protein 1 α (IRE1 α) which maintain their inactive state under normal conditions by binding to the protein chaperone glucose-regulated protein 78 (GRP78) in the ER lumen. However, following stimulation, GRP78 is removed from these sensors and activates the ER stress-associated signaling pathway (7). Endothelial cells stimulated by ox-LDL indicate an enhancement in the levels of the C/EBP α -homologous protein (CHOP) and caspase-12, which induce cell apoptosis (8), indicating that the ER stress levels have been abnormally elevated following ox-LDL stimulation. A previous study used an atherogenic rabbit model and demonstrated an increased expression of GRP78 in the endothelial layer of the aorta, as well as a significant increase in the levels of CHOP (9). The chronic glycolipid metabolic abnormalities induced the accumulation of adipose tissue, which was accompanied by high ER stress levels and was associated with NLRP3 inflammasome activation leading to vascular endothelial insulin resistance and exacerbating vascular damage (10). According to the aforementioned studies, the application of drugs that can inhibit ER stress can be used to restrain the formation of vascular injury-related diseases.

Statins act mainly by inhibiting the cholesterol synthetic pathway. It is hypothesized that statins may also have pleiotropic effects, such as reduction of the inflammatory process and esterification of cholesterol to macrophages (11). Therefore, the investigation of their extensive mechanism of action could potentially increase the efficacy of their therapeutic effects (12). Rosuvastatin has attracted considerable attention in its clinical application due to the significant reduction caused on LDL cholesterol levels compared with the effects of atorvastatin and simvastatin at the same dose (13). In addition, it remains unclear whether the endothelial and cardiovascular benefits of rosuvastatin are mediated by downregulating ER stress induced by dyslipidemia at cell or tissue level, which is independent of inhibiting cholesterol synthesis in atherosclerosis. Consequently, the present study investigated the effects of rosuvastatin on abnormal ER stress in human umbilical vascular endothelial cells (HUVECs) stimulated with ox-LDL and in aortic tissues of ApoE^{-/-} mice in order to explore the protective effects of this compound on endothelial cells.

Materials and methods

Chemical reagents. Human umbilical vein endothelial cells (HUVECs, CL-0122) and endothelial cell culture medium were

purchased from Procell Life Science & Technology Co., Ltd. Rosuvastatin (purity >98%; lot no. 511160104) was purchased from Lunan Better Pharmaceutical Co., Ltd. Ox-LDL (YB-002) was purchased from Guangzhou Yiyuan Biotechnologies Co., Ltd. Annexin V-FITC/ propidium iodide apoptosis detection kit (cat. no. C1062) and BCA protein assay kit were supplied by Beyotime Institute of Biotechnology. TRIzol[®] reagent was from Thermo Fisher Scientific, Inc. TransScript Green Two-Step RT-qPCR SuperMix (cat. no. AQ201-01) was from Beijing Transgen Biotech Co., Ltd. Caspase-12 fluorometric assay kit was from BioVision, Inc. An anti-eIF2 α polyclonal antibody (cat. no. BS3651), an anti-GRP78 polyclonal antibody (cat. no. BS1154) and an anti-PERK polyclonal antibody (cat. no. BS2156) were purchased from Bioworld Technology, Inc. An anti-phosphorylated (p-)eIF2 α (Ser 51) monoclonal antibody (3398) and an anti-IRE1 α monoclonal antibody (cat. no. 3294) were from Cell Signaling Technology, Inc. Anti-p-PERK (cat. no. 40294) polyclonal antibody and p-IRE1 α (cat. no. 16927) polyclonal antibody were obtained from Thermo Fisher Scientific, Inc. The anti-GAPDH monoclonal antibody (cat. no. TA-08), HRP-conjugated anti-rabbit IgG (cat. no. IH-0011) or anti-mouse IgG (cat. no. IH-0031), as well as primers of *CHOP*, *sXBP1* and *caspase-12* were from Beijing Dingguochangsheng Biotechnology Co., Ltd. LDL assay kit (cat. no. A113-1), high density lipoprotein (HDL) assay kit (cat. no. A112-1), total cholesterol (TC) assay kit (cat. no. A111-1) and triglyceride (TG) assay kit (cat. no. A110-1) were from Nanjing Jiancheng Bioengineering Institute.

Cell culture. HUVECs were cultured with endothelial cell culture medium (Ham's F-12K) supplemented contain 10% fetal bovine serum (FBS), 0.05 mg/ml endothelial cell growth supplement, 0.1 mg/ml heparin and 1% penicillin/streptomycin at 37°C and 5% CO₂.

Annexin V-FITC/ PI apoptosis assay. HUVECs in the logarithmic growth phase were dispersed by trypsinization, and seeded into 6-well plates at a density of 1x10⁵ cells/ml and 2 ml/well overnight at 37°C. Subsequently, HUVECs pretreated with the indicated concentration of rosuvastatin (0, 0.01, 0.1 and 1 μ mol/l) (14) for 24 h respectively; then, the cells were incubated with or without ox-LDL (200 μ g/ml) for another 24 h at 37°C. Following treatment, HUVECs were dispersed by trypsinization without any EDTA for 1 min and centrifuged at 1,000 x g for 5 min at 4°C. Sedimentary cells were washed by pre-cooled PBS three times and then resuspended in Annexin V-FITC combined liquid, 5 μ l Annexin V-FITC and 10 μ l PI added, and incubated for 20 min in dark with ice bath. The cell apoptosis amounts were detected with a flow cytometer (BD LSRFortessa, BD Biosciences) within 30 min, the values were calculated by BD FACSDiva[™] Software (v.8.0, BD Biosciences, Inc.).

Reverse transcription-quantitative (RT-q) PCR assay. HUVECs seeded into 6-well plates at a density of 1x10⁵ cells/ml and 2 ml/well overnight at 37°C, and cells in the logarithmic growth phase were treated with the indicated concentration of rosuvastatin and incubated with or without ox-LDL. Firstly, HUVECs were harvested and lysed in 1 ml TRIzol[®] reagent then mixed with 400 μ l chloroform by gently swirling. After

Table I. Sequence of amplified primers.

Primers	Forward	Reverse
<i>CHOP</i> (NM_001195057.1)	5'-GAACCAGGAAACGGAAACAG-3'	5'-ATTCACCATTTCGGTCAATCA-3'
<i>sXBP1</i> (NM_005080.3)	5'-GGATTCTGGCGGTATTGACT-3'	5'-AGGGAGGCTGGTAAGGAACT-3'
<i>Caspase-12</i> (NM_001191016.2)	5'-CAGCACATTCTGGTGTATTAT-3'	5'-GACTCTGGCAGTTACGGTTGTT-3'
<i>GAPDH</i> (NM_001289745.2)	5'-AGAAGGCTGGGGCTCATTG-3'	5'-AGGGGCCATCCACAGTCTTC-3'

resting for 5 min the mixture was centrifuged at 12,000 x g for 15 min at 4°C and 400 μ l of the upper aqueous phase collected. Isopropyl alcohol (400 μ l) was added and the mixture was centrifuged at 12,000 x g for 10 min at 4°C. The sedimentary RNA was washed with 75% ethanol, centrifuged at 12,000 x g for 5 min at 4°C, resuspended in DEPC water and the OD value detected at 260/280 nm (ratio 1.4-2.0). Subsequently, RNA was reverse-transcribed with oligo (dT) primers, and qPCR conducted with gene-specific primers in the presence of SYBR Premix Ex Taq (Beijing Transgen Biotech Co., Ltd.), the total reaction volume was 20 μ l. qPCR was conducted for three independent experiments, using *GAPDH* as the house-keeping control. The RT-qPCR amplification was performed with 40-60 cycles (95°C, 5 sec; 55°C, 15 sec; 72°C, 10 sec) with the oligonucleotide primer sets as in Table I. The relative expression levels of the target gene were calculated by the $2^{-\Delta\Delta C_q}$ method (15). All procedures were conducted according to the manufacturer's protocol.

Caspase-12 activity assay. HUVECs treated as previously described were harvested with cell lysis buffer on ice for 10 min, the protein concentration was determined with the BCA method and adjusted to equal amounts of protein samples. Cell lysates (50 μ l) were added into 96 well plates, then 50 μ l 2X reaction buffer containing 10 mmol/l DTT was added, as was 5 μ l ATAD-AFC buffer. After incubation for 1 h at 37°C, the OD value was measured at 405 nm and the relative activity of caspase-12 calculated. All samples were measured according to the manufacturer's protocol using a Hitachi 7150 Biochemical Autoanalyzer (Hitachi, Ltd.).

Western blot analysis. HUVECs in the logarithmic growth phase were treated with the indicated concentration of rosuvastatin, respectively, and incubated with or without ox-LDL. Then HUVECs were harvested in RIPA lysis buffer containing moderate protease inhibitor for 10 min on ice, and the protein concentration determined with the BCA method. The cell extract was centrifuged for 5 min at 14,000 x g and 4°C and equal amounts of protein samples (40 μ g) loaded onto 8-12% polyacrylamide-SDS gels. After electrophoresis, the gels were transferred to PVDF membranes which had been blocked with 5% (w/v) skimmed milk for 1 h at room temperature. Subsequently, the membranes were incubated with primary antibodies, including rabbit anti-eIF2 α polyclonal antibody (1:700), rabbit anti-p-eIF2 α (Ser 51) monoclonal antibody (1:1,000), rabbit anti-GRP78 polyclonal antibody (1: 700), rabbit anti-PERK polyclonal antibody (1:1,000), rabbit anti-p-PERK polyclonal antibody (1:1,500), rabbit anti-IRE1 α monoclonal antibody (1:1,000), rabbit

anti-p-IRE1 α monoclonal antibody (1:1,000) and mouse anti-GAPDH monoclonal antibody (1:5,000) at 4°C overnight. Finally, the bindings of target proteins were detected with secondary antibody conjugated to HRP (1:5,000) and visualized using ECL chemiluminescence (Beyotime Institute of Biotechnology), then calculated the densitometry with ImageJ software (version 1.51d; National Institutes of Health).

Atherosclerosis animal model protocol. ApoE^{-/-} male mice 20-22 g (n=16; 8 weeks old) were obtained from Beijing Vital River Laboratory Animal Technology and fed with atherogenic chow (a high-fat diet with 40 kcal% Fat, 1.25% Cholesterol), C57BL/6N male mice 20-22g (n=8; 8 weeks old) were purchased from Beijing Vital River Laboratory Animal Technology and fed normal chow as normal control. After atherogenic chow for 8 weeks, ApoE^{-/-} mice were randomly divided into two groups (n=8 each): Model group and rosuvastatin group (5 mg/kg). The rosuvastatin was dissolved in 0.5% carboxy methyl cellulose sodium and given once a day by intragastric administration; an equal volume of vehicle was given in the control and model groups for 4 weeks. Then the mice were euthanized using 20 mg/ml pentobarbital sodium (120 mg/kg body weight) through the intraperitoneal route, followed by cervical dislocation. During the present study, the animals were housed in a temperature of 22 \square 26 °C and a humidity of 50 \square 65% in a controlled environment with a 12-h light/dark cycle. The mice had free access to water and food, the padding was changed twice a week and the health status was observed with no mortalities. For animal welfare considerations, the mice were provided with tubular toys.

All the experiments *in vivo* were approved by the Animal Experimental Ethical Inspection Committee of Jilin University School of Pharmaceutical Sciences (ethical permission code: 20190025).

Measurement of LDL, HDL, TC and TG levels in serum. The mice were sacrificed following rosuvastatin treatment and the blood plasma was collected to detect LDL, HDL, TC and TG levels in serum. The methods of LDL and HDL detection were similar: 2.5 μ l serum from each group mice were added into 96 well plates, 2.5 μ l standard substance was also added as standard control and distilled water was used as a blank control; 180 μ l surfactant were added into each well for 5 min at 37°C and the OD value measured at 546 nm. Then 60 μ l surfactant 2 were added for 5 min at 37°C, the OD value was measured again and the concentration of LDL and HDL calculated. For the measurement of TC and TG, 2.5 μ l serum was

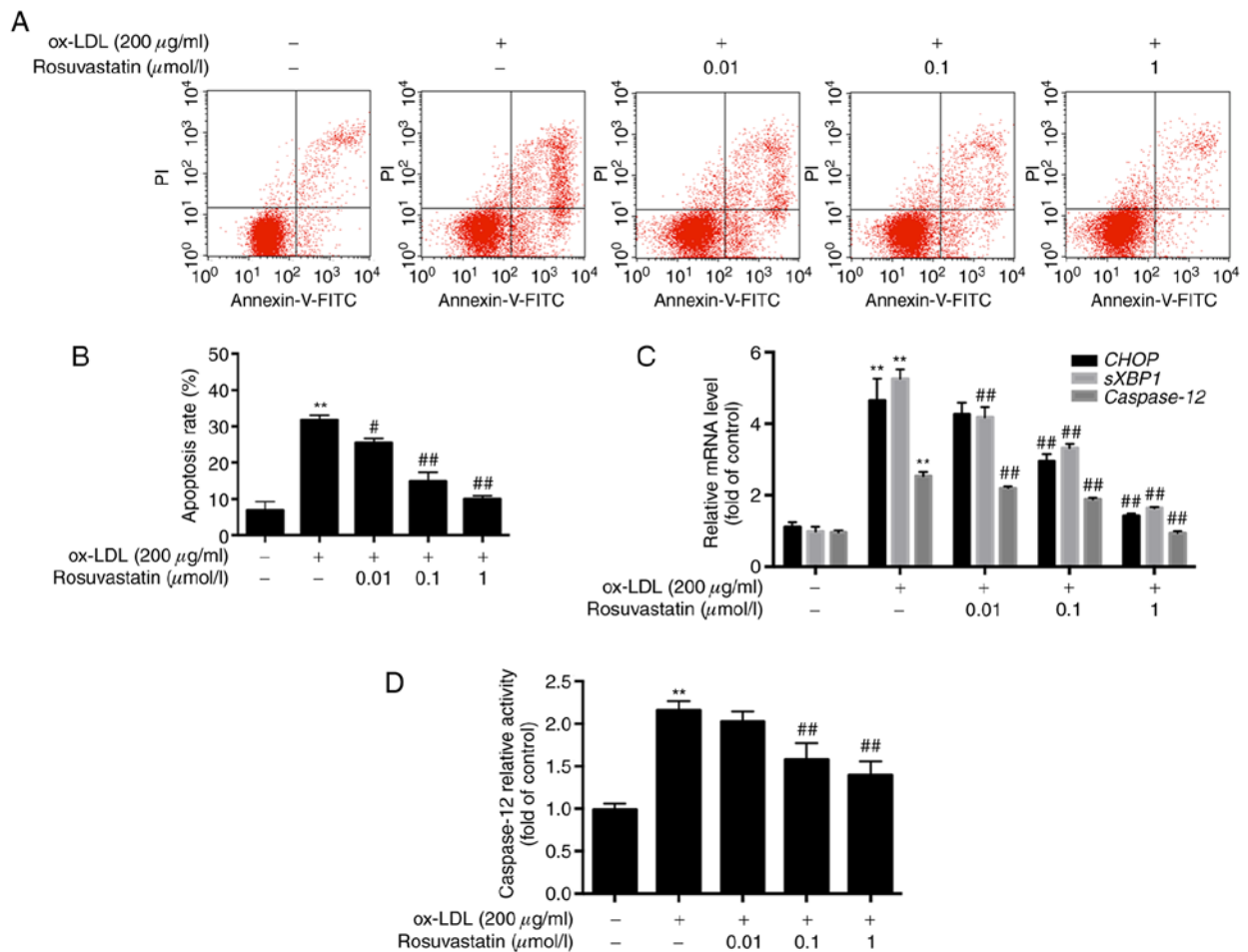


Figure 1. Effect of rosuvastatin on ox-LDL-induced HUVECs apoptosis. (A) Detection of apoptosis rate by flow cytometry. (B) The values of apoptosis rate analysis were expressed as the mean \pm standard deviation. (C) Effects of rosuvastatin on the mRNA levels of *CHOP*, *sXBP1*, *caspase-12* in HUVECs induced by ox-LDL. The fold of mRNA levels compared with control or ox-LDL group expressed as the mean \pm standard deviation. (D) Effects of rosuvastatin on the activity of caspase-12 in HUVECs induced by ox-LDL. The fold of caspase-12 activity compared with control or ox-LDL group expressed as the mean \pm standard deviation. ** $P < 0.01$ vs. control group; # $P < 0.05$ vs. ox-LDL group; ## $P < 0.01$ vs. ox-LDL group. ox-LDL, oxidized low-density lipoprotein; HUVECs, human umbilical vascular endothelial cells.

mixed with 250 μ l working fluid in 96-well plates for 10 min at 37°C, with standard substance as standard control and distilled water as a blank control; then the OD value was measured and the concentration of TC and TG calculated. All the samples were measured according to the manufacturer's protocol using a Hitachi 7150 Biochemical Autoanalyzer (Hitachi, Ltd.).

Histopathology and immunohistochemistry assays. The whole aorta was completely removed, the adipose tissue around the blood vessel peeled off, and the aorta dissected longitudinally with precision scissors prior to being fixed with 4% polyformaldehyde for 24 h at room temperature. Subsequently, the aortas were washed with PBS and 60% isopropanol, and stained in oil red O for 2 h in the dark at room temperature. Oil red O stained the lipid-rich plaque red. The aortas were smoothed on a black background and images captured; the total area and the red plaque area was calculated using ImageJ software (version 1.51d; National Institutes of Health).

The aortic root was dissected, removed, fixed in 4% polyformaldehyde for 48 h at room temperature, embedded in paraffin and cut into 5 μ m-thick sections. The sections were stained using a hematoxylin and eosin kit (Beyotime Institute of Biotechnology) for plaque morphology at

room temperature for 3 min. Other sections were blocked in 5% bovine serum albumin (BSA) at room temperature for 1 h and incubated with primary antibodies overnight at 4°C, then incubated with HRP-conjugated anti-rabbit IgG or anti-mouse IgG (1:5,000 dilution). TUNEL (1:9 mixed in equilibration buffer) staining of apoptotic cells was performed in the aorta for 1 h, and depicted as green fluorescence. DAPI (5 μ g/ml) dyed the nucleus for 5 min and showed blue fluorescence, and endomucin, the marker of endothelial cells, showed red fluorescence. All stains were performed at room temperature. Staining results were all observed and images captured under the routine microscope and fluorescence microscope, three fields per sample were observed, and analyzed using Photoshop (v.13.0; Adobe Systems, Inc.) and Image-Pro Plus 6 6.0 (Media Cybernetics, Inc.) analysis software.

Statistical analysis. Statistical analysis was performed using the SPSS v.22.0 statistical package (IBM Corp.). The results were expressed as the mean \pm standard deviation. Statistical differences among all groups were evaluated using one-way analysis of variance with Tukey's post hoc test. $P < 0.05$ was considered to indicate a statistically significant difference.

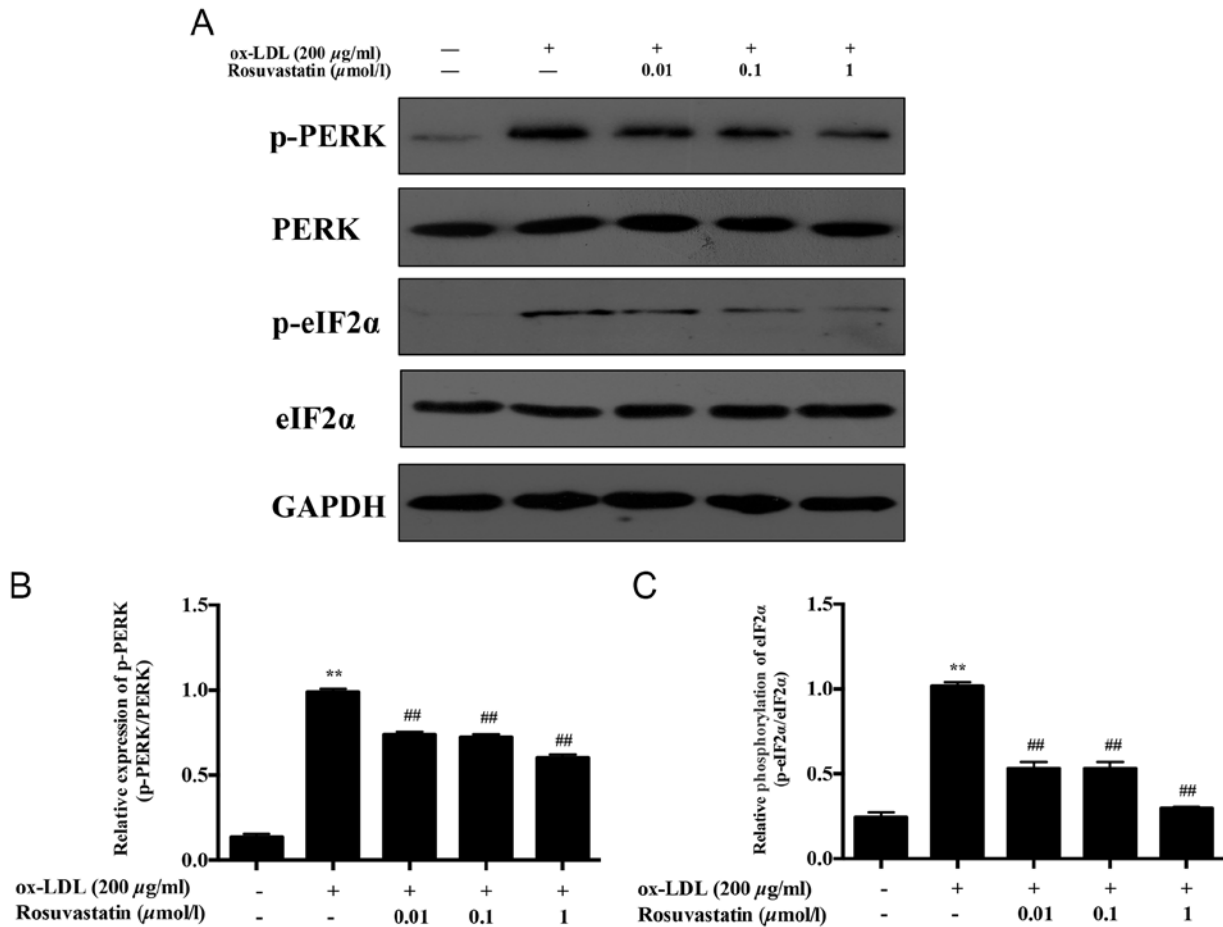


Figure 2. Effect of rosuvastatin on the phosphorylation of PERK and eIF2α in HUVECs induced by ox-LDL. (A) The expression of p-PERK and p-eIF2α in HUVECs. (B and C) The densitometric analysis of p-PERK and p-eIF2α, which expressed as the ratio of p-PERK/p-eIF2α to total PERK/eIF2α. GAPDH was the loading control. The densitometric analysis values expressed as the mean ± standard deviation. **P<0.01 vs. control group; ##P<0.01 vs. ox-LDL group. PERK, protein kinase RNA-like ER kinase; eIF2α, inositol-requiring protein 1α; HUVECs, human umbilical vascular endothelial cells; ox-LDL, oxidized low density lipoprotein; p-, phosphorylated.

Results

Effects of rosuvastatin on ox-LDL-induced HUVEC apoptosis. HUVECs were pretreated with rosuvastatin and the ox-LDL-mediated apoptotic rates were assessed by flow cytometry. HUVECs treated with ox-LDL (200 μg/ml) exhibited increased apoptosis. Specifically, the apoptotic rate of these cells was increased to 30.78±2.74% compared with that of the control cells (6.89±2.38%, P<0.01). However, the apoptotic rates of HUVECs, which were pretreated with rosuvastatin (0.01, 0.1 and 1 μmol/l), were decreased significantly in a concentration-dependent manner (P<0.01). The results suggested that rosuvastatin reversed the effects of ox-LDL-induced HUVEC apoptosis (Fig. 1A and B).

The results of the RT-qPCR analysis revealed that the mRNA levels of *CHOP*, *sXBPI* and *caspase-12* were all significantly increased in ox-LDL-stimulated HUVECs compared with those of the cells in the control group (P<0.01, Fig. 1C), while HUVECs pretreated with 0.1 and 1 μmol/l rosuvastatin exhibited lower mRNA levels of *CHOP* compared with those of the ox-LDL stimulated HUVECs (P<0.01). The mRNA levels of *sXBPI* and *caspase-12* in HUVECs pretreated with 0.01-1 μmol/l rosuvastatin were significantly

decreased in a concentration-dependent manner (P<0.01). Rosuvastatin decreased the mRNA levels of ER stress-associated apoptotic markers, suggesting that the inhibition of HUVEC apoptosis may be associated with the repression of ER stress hyperactivity. Furthermore, caspase-12 activity was increased in ox-LDL simulated HUVECs compared with the control (P<0.01, Fig. 1D), while 0.1 and 1 μmol/l rosuvastatin decreased caspase-12 activity in HUVECs compared with the ox-LDL stimulated group (P<0.01).

Effects of rosuvastatin on ER stress-associated signaling pathways in HUVECs induced with ox-LDL. The phosphorylation of PERK/eIF2α was proportional to the increase noted in the mRNA levels of *CHOP*. The phosphorylation levels of PERK and eIF2α were significantly increased in ox-LDL HUVECs (Fig. 2, P<0.01) compared with those in the ox-LDL stimulated group. HUVECs pretreated with 0.01 and 0.1 μmol/l rosuvastatin resulted in decreased expression levels of p-PERK (P<0.01), whereas 1 μmol/l rosuvastatin treatment caused a more evident decrease in the expression levels of p-PERK (P<0.01). The phosphorylation levels of eIF2α in HUVECs pretreated with 0.01 and 0.1 μmol/l rosuvastatin were decreased significantly (P<0.01). Treatment of the cells

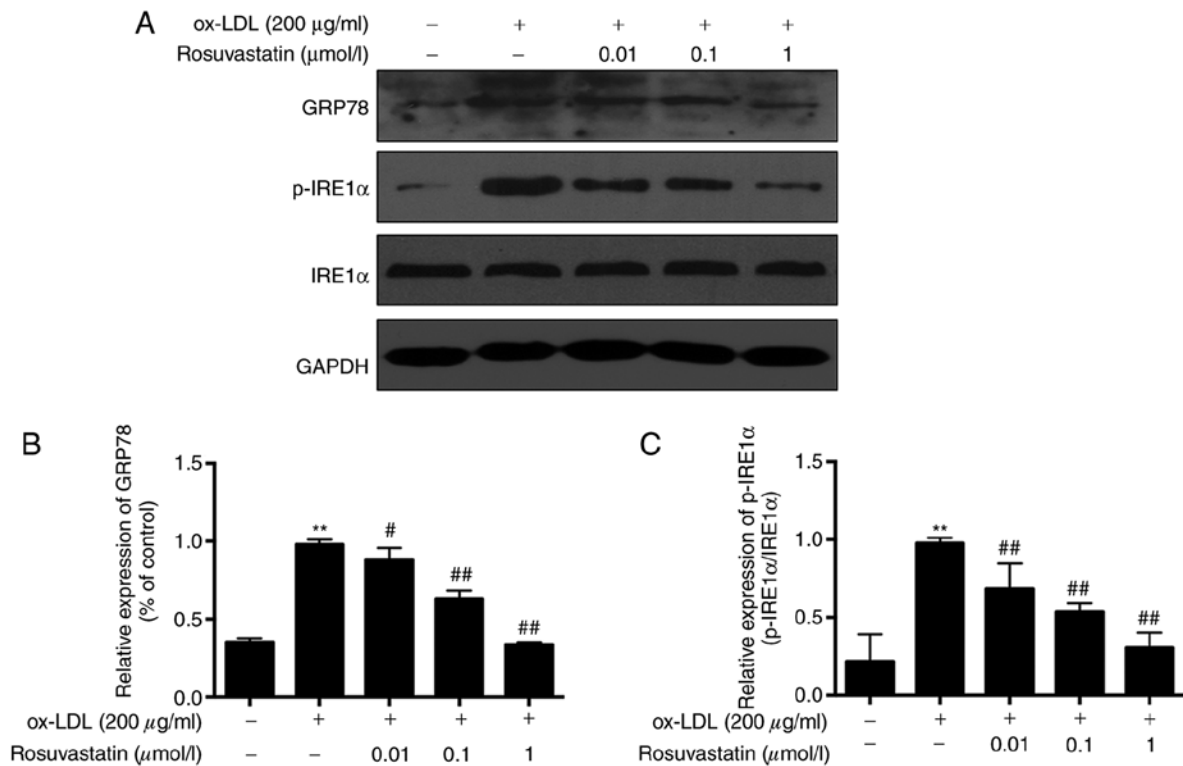


Figure 3. Effect of rosuvastatin on the expression of GRP78 and p-IRE1 α in HUVECs induced by ox-LDL. (A) The expression of GRP78 and p-IRE1 α in HUVECs. (B and C) The densitometric analysis of GRP78 and p-IRE1 α , the phosphorylation of IRE1 α expressed as the ratio of p-IRE1 α to total IRE1 α . GAPDH was the loading control and the subjacent band is the target band of GRP78. The densitometric analysis values expressed as the mean \pm standard deviation. ** $P < 0.01$ vs. control group; # $P < 0.05$ vs. ox-LDL; ## $P < 0.01$ vs. ox-LDL group. GRP78, glucose-regulated protein 78; p-, phosphorylated; IRE1 α , p-inositol-requiring protein 1 α ; HUVECs, human umbilical vascular endothelial cells.

with 1 $\mu\text{mol/l}$ rosuvastatin decreased the phosphorylation of eIF2 α significantly ($P < 0.01$), while the expression levels of total PERK and eIF2 α demonstrated no notable difference compared with those of the control or ox-LDL induced HUVECs.

Concomitantly, the expression levels of ER-stress sensor proteins, including GRP78 and p-IRE1 α were investigated. The levels of GRP78 and p-IRE1 α in ox-LDL simulated HUVECs were significantly increased compared with those of the control group (Fig. 3, $P < 0.01$). Following treatment of the cells with rosuvastatin at a concentration range of 0.01-1 $\mu\text{mol/l}$, the GRP78 and p-IRE1 α levels were decreased in a concentration-dependent manner ($P < 0.01$). The results suggested that rosuvastatin protected ox-LDL-induced HUVEC apoptosis by repressing the ER stress.

Effects of rosuvastatin on atherogenesis induced by high-fat diet in ApoE $^{-/-}$ mice. Initially, the serum lipoprotein levels were detected in each group of mice. Specifically, the serum LDL, TC and TG levels of the model mice that were induced by high-fat diet were significantly higher compared with those of the normal mice ($P < 0.01$; Table II), whereas the HDL levels were significantly reduced ($P < 0.01$). Rosuvastatin treatment significantly changed the levels of LDL and TG compared with those in the model group ($P < 0.05$), while the effects of rosuvastatin on HDL and TC were not apparent.

The vascular intima of the normal mice was smooth without atherosclerotic plaques, while a high number of atherosclerotic plaques were noted in the aorta intima of ApoE $^{-/-}$ mice fed

with atherogenic chow for 12 weeks ($P < 0.01$). These data indicated that the atherosclerosis model was successful and that rosuvastatin significantly alleviated aortic plaque deposition compared with that of the model group ($P < 0.01$). In addition, the cross-section lesion areas were significantly increased in the model group compared with those of the normal group ($P < 0.01$). The lesions were significantly decreased in the rosuvastatin-treated group ($P < 0.01$, Fig. 4A and B).

Effect of rosuvastatin on aortic endothelial cell apoptosis. Endomucin is the marker of endothelial cells and is stained with red fluorescence. A large amount of aortic endothelial cell apoptosis was noted in atherosclerotic ApoE $^{-/-}$ mice compared with normal mice ($P < 0.01$; Fig. 5), whereas the induction of endothelial cell apoptosis was significantly reduced following treatment of the cells with rosuvastatin ($P < 0.01$). These results indicated that rosuvastatin could inhibit apoptosis of vascular endothelial cells induced by high-fat diet.

Effect of rosuvastatin on ER stress in the aortic intima of atherosclerotic mice. The expression levels of GRP78, p-PERK, p-IRE1 α and p-eIF2 α were investigated in the aortic intima of ApoE $^{-/-}$ mice. GRP78, p-PERK, p-IRE1 α and p-eIF2 α were rarely expressed in the aorta intima of normal mice compared with the strong expression which was noted in the intima and plaque of model mice ($P < 0.01$; Fig. 6). Rosuvastatin inhibited the expression levels of the ER stress signaling pathway proteins and decreased significantly the expression levels of phosphorylated PERK, IRE1 α and eIF2 α ($P < 0.05$). The results

Table II. Serum LDL, HDL, TC and TG levels of each group of mice.

Group	LDL (mmol/l)	HDL (mmol/l)	TC (mmol/l)	TG (mmol/l)
Control	0.41±0.24	2.72±0.49	5.32±1.60	1.32±0.43
Model	16.43±3.89 ^a	1.73±0.39 ^a	66.50±7.91 ^a	7.57±1.74 ^a
Rosuvastatin	12.49±1.71 ^b	1.98±0.29	59.59±11.63	5.65±1.16 ^b

^aP<0.01 vs. Control group; ^bP<0.05 vs. Model group. LDL, low density lipoprotein; HDL, high density lipoprotein; TC, total cholesterol; TG, triacylglycerol.

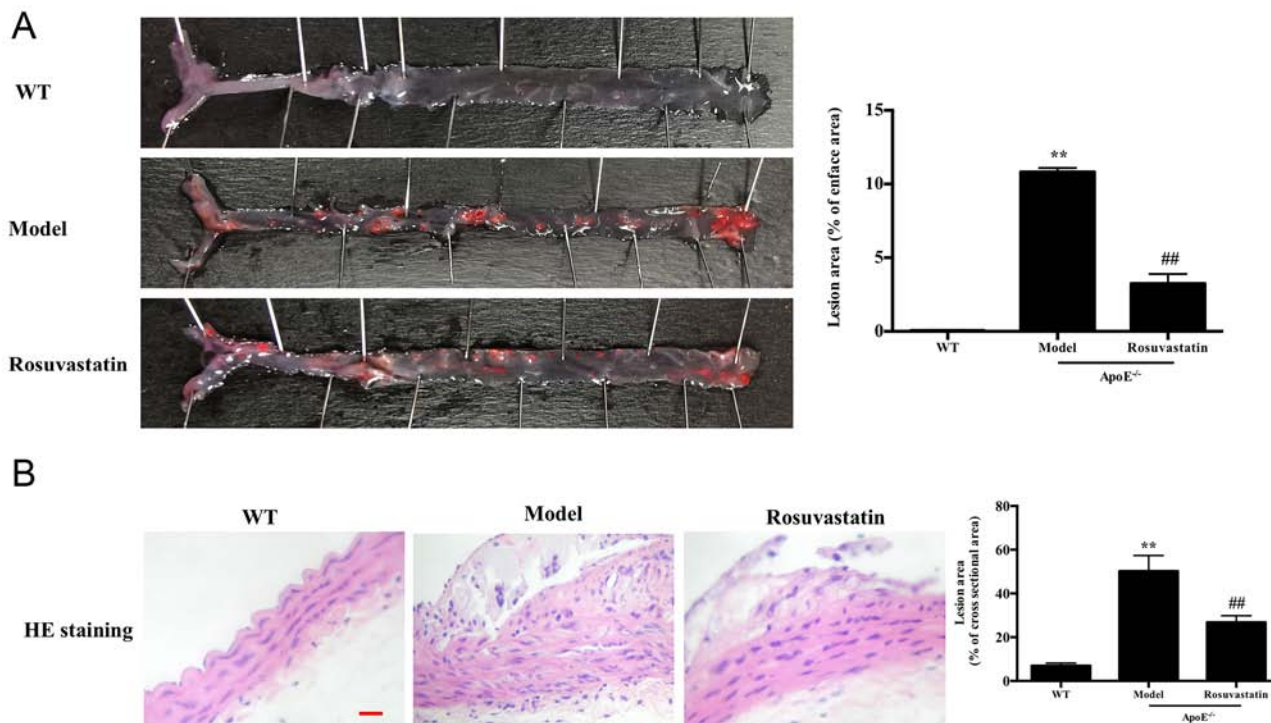


Figure 4. Effect of rosuvastatin on atherosclerosis in aorta of ApoE^{-/-} mice induced by high-fat diet. (A) Oil red O staining of total aorta. Lesion area (%) = (plaque area/total area of aorta) x 100%. The values expressed as the mean ± standard deviation. (B) Representative HE staining of aortic cross sections, magnification, x 400, scale bar = 50 μm. **P<0.01 vs. Control group; ##P<0.01 vs. Model group. HE, hematoxylin and eosin.

indicated that rosuvastatin could inhibit ER stress in vascular endothelial cells treated with a high-fat diet.

Discussion

Atherosclerosis has attracted considerable attention worldwide, due to its high risk of mortality in cardiovascular and cerebrovascular diseases (16). The disruption of lipid metabolism is critical for the formation of atherosclerosis (17). Vascular endothelial cells can limit the atherosclerotic process by resisting inflammatory cell infiltration, which mainly results in the formation of the atherosclerotic plaques (18). Dyslipidemia covers a wide range of lipoprotein abnormalities, including abnormal levels of LDL, TC, TG and HDL. LDL receptors are first upregulated in cholesterol metabolism (19), and LDL ingested and modified into ox-LDL exhibits a variety of proatherogenic properties on cultured vascular cells (20). Thus the intervention of ox-LDL for vascular cells in study of AS

in vitro is widely used (21). In the present study, HUVECs were incubated with ox-LDL *in vitro*, which caused the induction of apoptosis as determined by flow cytometry. Furthermore, the cytotoxicity of ox-LDL and its ability to promote endothelial cell apoptosis was significantly increased leading to atherosclerotic plaque instability and rupture (22). The present study further indicated that a high-fat diet led to significantly abnormal blood lipids and severe atherosclerotic pathological changes in ApoE^{-/-} mice. These alterations included disorder in endothelial cell arrangement and the formation of aortic plaques in the aorta intima, as well as a large fraction of endothelial cell apoptosis. The results suggested severe endothelial cell injury during atherosclerosis.

ER stress induced by ox-LDL is an important mechanism of endothelial cell apoptosis that includes upregulation of the PERK/eIF2α/CHOP signaling pathway, as well as the cleavage of caspase-3. These processes are associated with ER stress-induced apoptosis (23) and a variety of key lipid synthesis

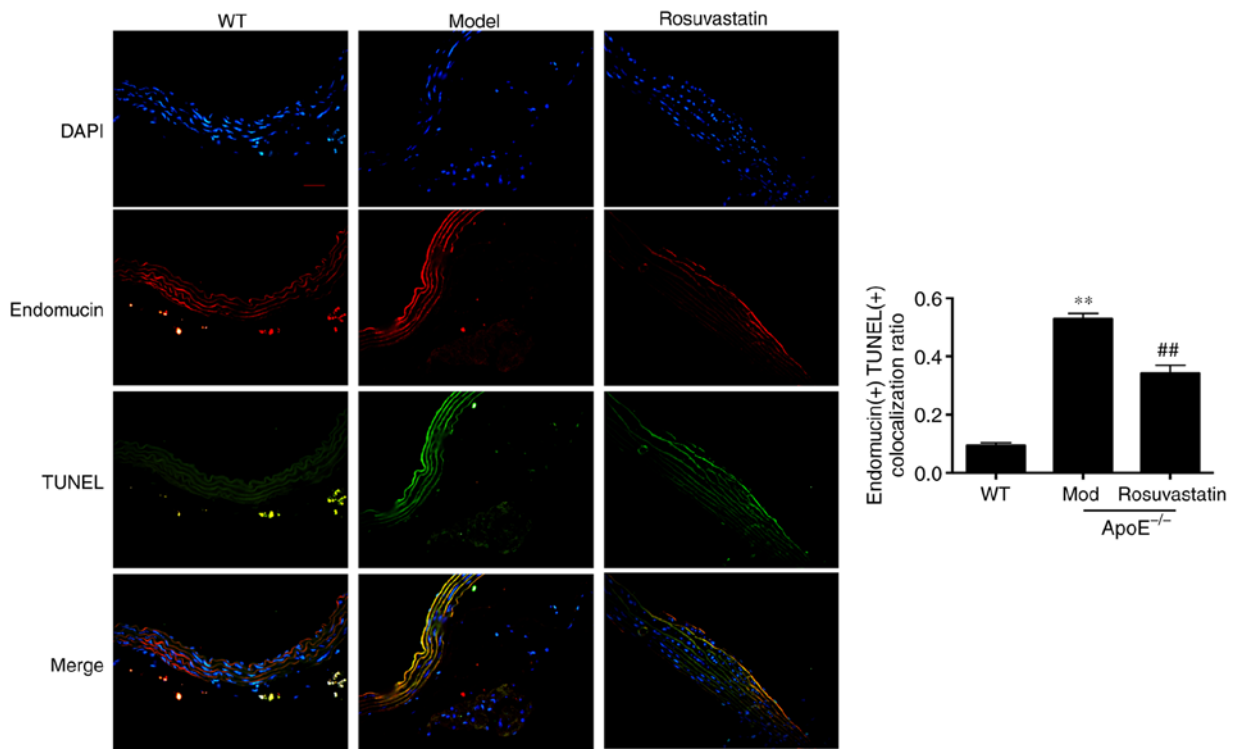


Figure 5. Effect of rosuvastatin on aortic endothelial cell apoptosis. Representative immunofluorescence staining of aortic cross sections. Endomucin⁽⁺⁾/TUNEL⁽⁺⁾ colocalization ratio were counted and expressed as the mean \pm standard deviation. Magnification, x 200, scale bar = 100 μ m. **P<0.01 vs. Control group; ##P<0.01 vs. Model group.

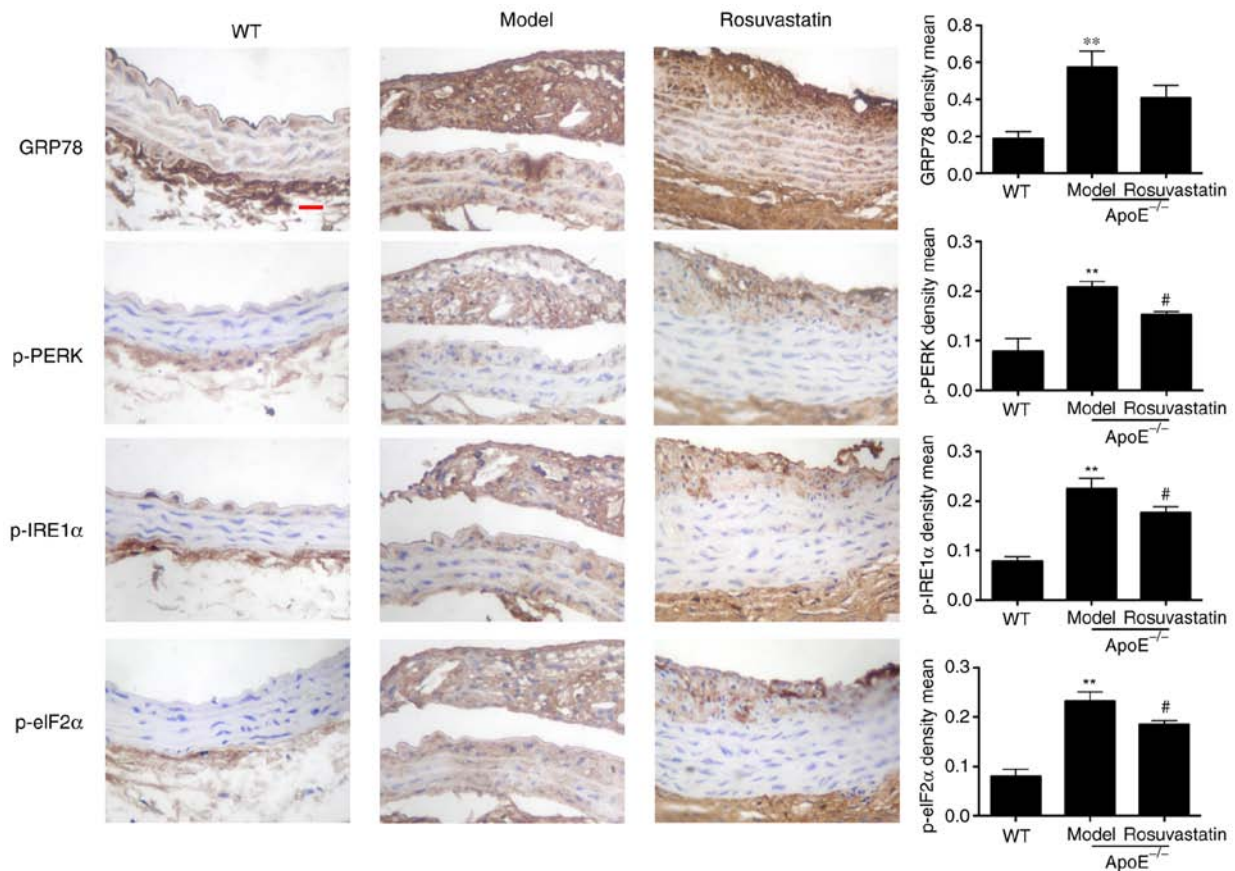


Figure 6. Effect of rosuvastatin on ER stress in aortic intima of atherosclerotic mice. Representative immunohistochemical staining and content quantification of GRP78, p-PERK, p-IRE1 α and p-eIF2 α in aortic intima and plaque, magnification, x 400, scale bar = 50 μ m. The density means expressed as the mean \pm standard deviation. **P<0.01 vs. Control group; #P<0.01 vs. Model group. ER GRP78, glucose-regulated protein 78; p-, phosphorylated; PERK, protein kinase RNA-like ER kinase; IRE1 α , p-inositol-requiring protein 1 α ; eIF2 α , inositol-requiring protein 1 α .

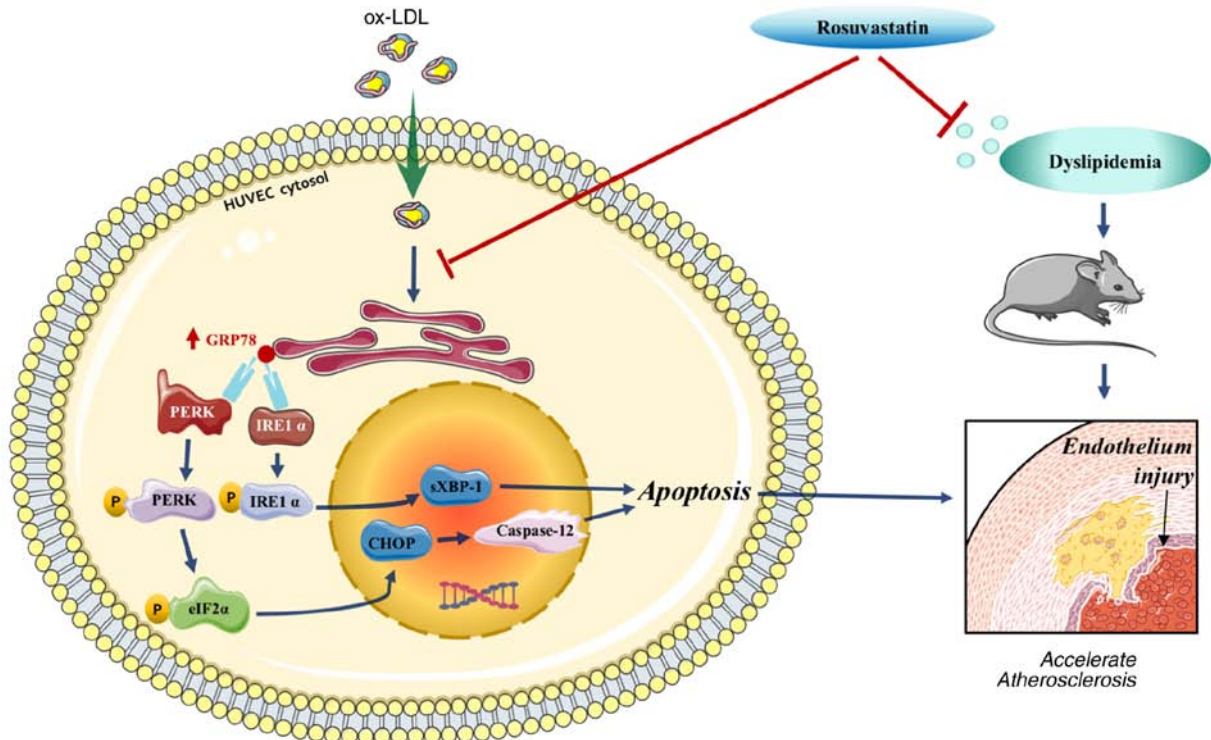


Figure 7. Schematic overview shows that rosuvastatin reverse the HUVECs apoptosis triggered by ox-LDL and endothelial injury induced by high-fat diets specifically by downregulating PERK/p-eIF2 α /CHOP and IRE1 α /sXBP1 signaling pathways.

pathways are located in the ER, which means dyslipidemia can specifically stimulate abnormally high ER levels associated with apoptosis (24). A previous study indicated that ER functions are not only required for the regulation of lipid metabolic disorders in the liver, but they can also protect from endothelial cell homeostasis, since increased levels of lipids can disturb ER homeostasis, leading to ER stress and vascular injury (25). Under the electron microscope, vascular endothelial cells can be observed with highly developed ER, which suggests that endothelial cells are more sensitive to ER (5,26). The exposure of endothelial cells to ox-LDL induces a time-dependent dissociation of PERK and GRP78 in human atherosclerotic lesions that leads to splicing of *IRE1 α* mRNA, which encodes for the X-box-binding protein-1 (*sXBP1*) (24). In addition, upregulated mRNA levels of *caspase-12* are noted, which is the specific apoptotic factor activated by ER stress (8). The present study indicated that ox-LDL induced a considerable increase in the mRNA levels of *sXBP1* and *caspase-12*, along with *caspase-12* relative activity, indicating that ox-LDL could induce ER stress-associated apoptosis. Notably, PERK activated its specific downstream marker eIF2 α , which played a key role in upregulating the mRNA levels of *CHOP*, thereby repressing ER stress-associated apoptosis in highly active secretory endotheliocytes. This pathway could be considered an important target for vascular protection (27). In the present study, the ox-LDL-stimulated group demonstrated a significant increase in the mRNA levels of *CHOP* and in the phosphorylation of eIF2 α , which was consistent with a previous study (8). Notably, the levels of the characteristic protein of ER stress, GRP78, were significantly increased, whereas PERK and IRE1 α were highly phosphorylated. ER stress has recently been identified as not only an important mechanism of endothelial cell apoptosis, but also as a key risk factor to plaque growth and

instability in atherosclerosis (22). The present study indicated high expression levels of GRP78, as well as p-PERK, IRE1 α and eIF2 α in the aortic intimal plaque of atherosclerotic mice, indicating that ER stress was overactivated. In addition, ER is the pivotal storage site of intracellular Ca²⁺ and can accelerate the biosynthesis of cholesterol in animals (28). Insufficient levels of Ca²⁺ induce abnormal protein folding in ER by inhibiting PCSK9 secretion, which can in turn degrade LDL receptor-dependent cholesterol uptake in hepatocytes, thereby resulting in disturbed lipid metabolism (29). Various pathological conditions including homocysteinemia, hyperlipidemia, high glucose levels and insulin resistance can lead to endothelial dysfunction in part through the activation of ER stress (30). Previous studies have reported effects of statins on homocysteine and high glucose-induced endothelial ER stress at the cellular level (31,32). However, statins can induce new onset diabetes mellitus, especially in subjects prone to diabetes, which cannot be ignored (33). Therefore, the inhibition of endothelial injury and apoptosis induced by ER stress is considered a therapeutic strategy for the prevention of atherosclerosis.

Rosuvastatin is an inhibitor of HMG-CoA reductase, which reduces cholesterol levels in the circulation by restricting the generation of cholesterol precursors and stimulating catabolism of LDL (26). This is achieved by enhancing the expression of the LDL receptor in the hepatocyte surface (34). By contrast, statins exhibit multiple effects on atherosclerosis, rosuvastatin can control the process of atherosclerotic cerebral infarction (ACI) in patients, which is associated with inhibition of the expression of OX40 ligand and the stimulation of the expression of PPAR- γ in endothelial cells (35); however, few studies have been performed on ER stress induced by dyslipidemia in endothelial cells. To this end, it was hypothesized that inhibition of ER stress

may be another important protective mechanism of rosuvastatin in aortic endothelium. Ox-LDL-stimulated HUVECs were pretreated with 0.01-1 $\mu\text{mol/l}$ rosuvastatin and the induction of cell apoptotic rates indicated a marked decrease compared with that noted in ox-LDL-treated cells. The mRNA levels of *CHOP*, *sXBP1* and *caspase-12* in rosuvastatin pretreated groups were notably suppressed following the increase in rosuvastatin concentration and the caspase-12 activity was clearly decreased. Notably, the expression levels of GRP78 and the phosphorylation levels of PERK, IRE1 α and eIF2 α were all decreased by rosuvastatin treatment in a concentration-dependent manner. Furthermore, atherosclerotic mice were orally treated with rosuvastatin and the incidence of the aortic plaque in aortic intima was reduced. In addition, LDL and TG levels in the serum were significantly reduced, along with the induction of apoptosis in aortic endotheliocytes. The expression levels of the phosphorylated proteins PERK, IRE1 α and eIF2 α were significantly inhibited in the aorta intima, which verified the protective effect of rosuvastatin on endothelium. A previous study demonstrated that statins exert 'pleiotropic' therapeutic effects and can be used in extensive clinical applications (36). The use of statins can protect against liver cirrhosis and fibrosis by ameliorating the dysfunction of hepatic endothelial cells via the upregulation of KLF-2 expression (37), as well as the inhibition of endothelial cell dysfunction, which is induced by chronic intermittent hypoxia in obstructive sleep apnea patients. These subjects did not exhibit comorbidities, such as high levels of LDL and obesity, which could potentially increase coronary vascular risk and stroke (38). For future studies, it is intended to perform microarray detection and bioinformatics analysis of mouse aorta to screen out which upstream proteins, microRNA or long non-coding RNA may be involved in the regulation of ER stress apoptosis by rosuvastatin, and further verify the possible upstream factors in ox-LDL-induced endothelial cells, which may contribute to the design of novel therapeutic strategies that target the vascular endothelium for the prevention and treatment of endothelial dysfunction-associated diseases.

In conclusion, rosuvastatin reversed HUVEC apoptosis, which was triggered by ox-LDL and endothelial injury induced by a high-fat diet. These processes were mediated by downregulating the PERK/p-eIF2 α /CHOP and IRE1 α /sXBP1 signaling pathways (Fig. 7), indicating that rosuvastatin may be conducive to enhance endothelial function. The data suggested that rosuvastatin can be applied to the treatment of other endothelial dysfunction-related diseases.

Acknowledgements

Not applicable.

Funding

The present study was supported by the Science and Technology Development Projects of Jilin, China (grant no. 20150101200JC).

Availability of data and materials

The datasets used and/or analyzed during the present study are available from the corresponding author on reasonable request.

Authors' contributions

HX, DS and GL conceived and designed the study. JG, HX, WF and XY performed the experiments. JG, DS and HX wrote the paper. GX and HC analyzed the data. DS reviewed and edited the manuscript. All authors read and approved the final manuscript.

Ethics approval and consent to participate

All the animal experiments were approved by the Animal Experimental Ethical Inspection Committee of Jilin University School of Pharmaceutical Sciences (ethical permission code: 20190025).

Patient consent for publication

Not applicable

Competing interests

The authors declare that they have no competing interests.

References

- Hald EM, Lijfering WM, Mathiesen EB, Johnsen SH, Løchen ML, Njølstad I, Wilsgaard T, Rosendaal FR, Brækkan SK and Hansen JB: Carotid atherosclerosis predicts future myocardial infarction but not venous thromboembolism: The Tromsø study. *Arterioscler Thromb Vasc Biol* 34: 226-230, 2014.
- Byfield FJ, Tikku S, Rothblat GH, Gooch KJ and Levitan I: OxLDL increases endothelial stiffness, force generation, and network formation. *J Lipid Res* 47: 715-723, 2006.
- Sarvani C, Sireesh D and Ramkumar KM: Unraveling the role of ER stress inhibitors in the context of metabolic diseases. *Pharmacol Res* 119: 412-421, 2017.
- Wu MY, Li CJ, Hou MF and Chu PY: New insights into the role of inflammation in the pathogenesis of atherosclerosis. *Int J Mol Sci* 18: 2034, 2017.
- Luchetti F, Crinelli R, Cesarini E, Canonico B, Guidi L, Zerbinati C, Di Sario G, Zamai L, Magnani M, Papa S, *et al*: Endothelial cells, endoplasmic reticulum stress and oxysterols. *Redox Biol* 13: 581-587, 2017.
- Klausner RD and Sitia R: Protein degradation in the endoplasmic reticulum. *Cell* 62: 611-614, 1990.
- Zhou AX and Tabas I: The UPR in atherosclerosis. *Semin Immunopathol* 35: 321-332, 2013.
- Hong D, Bai YP, Gao HC, Wang X, Li LF, Zhang GG and Hu CP: Ox-LDL induces endothelial cell apoptosis via the LOX-1-dependent endoplasmic reticulum stress pathway. *Atherosclerosis* 235: 310-317, 2014.
- Kruzliak P, Sabo J and Zulli A: Endothelial endoplasmic reticulum and nitrate stress in endothelial dysfunction in the atherogenic rabbit model. *Acta Histochem* 117: 762-766, 2015.
- Xu X, Chen Y, Song J, Hou F, Ma X, Liu B and Huang F: Mangiferin suppresses endoplasmic reticulum stress in perivascular adipose tissue and prevents insulin resistance in the endothelium. *Eur J Nutr* 57: 1563-1575, 2018.
- Egom EE, Pharithi RB, Hesse S, Starr N, Armstrong R, Sulaiman HM, Gazdikova K, Mozos I, Caprnda M, Kubatka P, *et al*: Latest updates on lipid management. *High Blood Press Cardiovasc Prev* 26: 85-100, 2019.
- Breder I, Coope A, Arruda AP, Razolli D, Milanski M, Dorigheo GG, de Oliveira HC and Velloso LA: Reduction of endoplasmic reticulum stress--a novel mechanism of action of statins in the protection against atherosclerosis. *Atherosclerosis* 212: 30-31, 2010.
- Karlson BW, Palmer MK, Nicholls SJ, Lundman P and Barter PJ: A VOYAGER meta-analysis of the impact of statin therapy on low-density lipoprotein cholesterol and triglyceride levels in patients with hypertriglyceridemia. *Am J Cardiol* 117: 1444-1448, 2016.

14. Geng J, Xu H, Yu X, Xu G, Cao H, Lin G and Sui D: Rosuvastatin protects against oxidized low-density lipoprotein-induced endothelial cell injury of atherosclerosis in vitro. *Mol Med Rep* 19: 432-440, 2019.
15. Livak KJ and Schmittgen TD: Analysis of relative gene expression data using real-time quantitative PCR and the 2(-Delta Delta C(T)) Method. *Methods* 25: 402-408, 2001.
16. Tugcu A, Jin Z, Homma S, Elkind MS, Rundek T, Yoshita M, DeCarli C, Nakanishi K, Shames S, Wright CB, *et al*: Atherosclerotic plaques in the aortic arch and subclinical cerebrovascular disease. *Stroke* 47: 2813-2819, 2016.
17. Li D, Zhang L, Dong F, Liu Y, Li N, Li H, Lei H, Hao F, Wang Y, Zhu Y, *et al*: Metabonomic changes associated with atherosclerosis progression for LDLR(-/-) mice. *J Proteome Res* 14: 2237-2254, 2015.
18. Rafieian-Kopaei M, Setorki M, Douidi M, Baradaran A and Nasri H: Atherosclerosis: Process, indicators, risk factors and new hopes. *Int J Prev Med* 5: 927-946, 2014.
19. Goldstein JL and Brown MS: A century of cholesterol and coronaries: From plaques to genes to statins. *Cell* 161: 161-172, 2015.
20. Goyal T, Mitra S, Khaidakov M, Wang X, Singla S, Ding Z, Liu S and Mehta JL: Current concepts of the role of oxidized LDL receptors in atherosclerosis. *Curr Atheroscler Rep* 14: 150-159, 2012.
21. Zhong X, Ma X, Zhang L, Li Y, Li Y and He R: MIAT promotes proliferation and hinders apoptosis by modulating miR-181b/STAT3 axis in ox-LDL-induced atherosclerosis cell models. *Biomed Pharmacother* 97: 1078-1085, 2018.
22. Nègre-Salvayre A, Augé N, Camaré C, Bacchetti T, Ferretti G and Salvayre R: Dual signaling evoked by oxidized LDLs in vascular cells. *Free Radic Biol Med* 106: 118-133, 2017.
23. Tao YK, Yu PL, Bai YP, Yan ST, Zhao SP and Zhang GQ: Role of PERK/eIF2 α /CHOP endoplasmic reticulum stress pathway in oxidized low-density lipoprotein mediated induction of endothelial apoptosis. *Biomed Environ Sci* 29: 868-876, 2016.
24. Sanson M, Augé N, Vindis C, Muller C, Bando Y, Thiers JC, Marachet MA, Zarkovic K, Sawa Y, Salvayre R, *et al*: Oxidized low-density lipoproteins trigger endoplasmic reticulum stress in vascular cells: Prevention by oxygen-regulated protein 150 expression. *Circ Res* 104: 328-336, 2009.
25. Röhrl C and Stangl H: Cholesterol metabolism-physiological regulation and pathophysiological deregulation by the endoplasmic reticulum. *Wien Med Wochenschr* 168: 280-285, 2018.
26. Dong Y, Fernandes C, Liu Y, Wu Y, Wu H, Brophy ML, Deng L, Song K, Wen A, Wong S, *et al*: Role of endoplasmic reticulum stress signalling in diabetic endothelial dysfunction and atherosclerosis. *Diab Vasc Dis Res* 14: 14-23, 2017.
27. Dickhout JG, Hossain GS, Pozza LM, Zhou J, Lhoták S and Austin RC: Peroxynitrite causes endoplasmic reticulum stress and apoptosis in human vascular endothelium: Implications in atherogenesis. *Arterioscler Thromb Vasc Biol* 25: 2623-2629, 2005.
28. Fu XL and Gao DS: Endoplasmic reticulum proteins quality control and the unfolded protein response: The regulative mechanism of organisms against stress injuries. *Biofactors* 40: 569-585, 2014.
29. Lebeau P, Al-Hashimi A, Sood S, Lhoták Š, Yu P, Gyulay G, Paré G, Chen SR, Trigatti B, Prat A, *et al*: Endoplasmic reticulum stress and Ca²⁺ depletion differentially modulate the sterol-regulatory protein PCSK9 to control lipid metabolism. *J Biol Chem* 292: 1510-1523, 2017.
30. Lenna S, Han R and Trojanowska M: Endoplasmic reticulum stress and endothelial dysfunction. *IUBMB Life* 66: 530-537, 2014.
31. Jia F, Wu C, Chen Z and Lu G: Atorvastatin inhibits homocysteine-induced endoplasmic reticulum stress through activation of AMP-activated protein kinase. *Cardiovasc Ther* 30: 317-325, 2012.
32. Zhao SP, Wu ZH, Wu J, Hong SC and Deng P: Effect of atorvastatin on tumor necrosis factor alpha serum concentration and mRNA expression of adipose in hypercholesterolemic rabbits. *J Cardiovasc Pharmacol* 46: 185-189, 2005.
33. Chrysant SG: New onset diabetes mellitus induced by statins: Current evidence. *Postgrad Med* 129: 430-435, 2017.
34. Raghov R: Statins redux: A re-assessment of how statins lower plasma cholesterol. *World J Diabetes* 8: 230-234, 2017.
35. Zhang JY, Liu B, Wang YN, Zhang WN and Wang FJ: Effect of rosuvastatin on OX40L and PPAR- γ expression in human umbilical vein endothelial cells and atherosclerotic cerebral infarction patients. *J Mol Neurosci* 52: 261-268, 2014.
36. Adhyaru BB and Jacobson TA: Safety and efficacy of statin therapy. *Nat Rev Cardiol* 15: 757-769, 2018.
37. Vargas JI, Arrese M, Shah VH and Arab JP: Use of statins in patients with chronic liver disease and cirrhosis: Current views and prospects. *Curr Gastroenterol Rep* 19: 43, 2017.
38. Toraldo DM, Benedetto M, Conte L and De Nuccio F: Statins may prevent atherosclerotic disease in OSA patients without co-morbidities? *Curr Vasc Pharmacol* 15: 5-9, 2017.



This work is licensed under a Creative Commons Attribution-NonCommercial-NoDerivatives 4.0 International (CC BY-NC-ND 4.0) License.